CrystEngComm

Cite this: *CrystEngComm*, 2011, **13**, 5239

www.rsc.org/crystengcomm

**PAPER**

# High temperature Raman spectroscopy study on the microstructure of the boundary layer around a growing $LiB_3O_5$ crystal

**Di Wang,[a] Songming Wan,*[ab] Shaotang Yin,*[a] Qingli Zhang,[a] Jinglin You,[b] Guochun Zhang[c] and Peizhen Fu[c]**

***Received 28th March 2011, Accepted 23rd May 2011***
**DOI: 10.1039/c1ce05375b**



High temperature Raman spectroscopy has been applied to investigate *in situ* the microstructure of the high temperature solution near a $LiB_3O_5$ (LBO) crystal–solution interface. A preordering boundary layer was found around the interface. In the boundary layer, an isomerization reaction between 3-coordinated and 4-coordinated boron was observed. The reaction led to the formation of $B_3Ø_7$ triborate groups, the characteristic structural group involved in the LBO crystal. According to the mechanism, the growth habits of LBO crystal can be understood well.

## Introduction

During crystal growth, a boundary layer is believed to form in the liquid phase zone adjacent to the crystal–liquid interface; it has a different component to the bulk liquid.[1] Recent studies on the growth mechanisms of some borate crystals have proved that the boundary layer also has a different microstructure to the bulk liquid,[2–5] and the microstructure is essential for understanding the crystal growth mechanism and for interpreting the crystal growth habits.[6,7] The previous works all focused on the microstructure of the boundary layer in congruent systems in which the component of the crystal is identical to that of the liquid phase. For the crystals that melt incongruently or suffer from phase transition in the cooling process, a high-temperature solution growth technique (flux growth technique) is the most suitable method to obtain large and high quality single crystals.[8] However, few reports can be found in the literature on the microstructure of the boundary layer in the flux system; therefore, it is an important and interesting issue to study.

Lithium borate ($LiB_3O_5$, LBO), one of the five stable compounds in the $Li_2O$–$B_2O_3$ system,[9,10] has been extensively applied in nonlinear optical devices due to its excellent nonlinear optical properties.[11] According to the $Li_2O$–$B_2O_3$ binary phase diagram,[9] LBO crystal melts incongruently at 834 °C, and can be grown by the flux method using the self-flux $B_2O_3$.[12] In the past few decades, most studies have concentrated on its growth conditions, defects and growth habit.[12–15] Although several researches on the LBO crystal growth mechanism have been reported, yet the conclusions are based on the conjectural structure obtained from the glass with identical composition to the high-temperature solution rather than on the reliable microstructure of the high-temperature solution obtained from *in situ* investigation.

It is difficult to investigate *in situ* the microstructure of the boundary layer because the thickness of the boundary layer usually is less than 100 μm and the investigation should be carried out at high temperature. With the advantages of *in situ* observation, microscale analysis, and high-temperature measurement, high temperature Raman spectroscopy is a suitable tool to study the microstructure of the boundary layer.[16,17] In this work, high temperature Raman spectroscopy is applied to investigate *in situ* the microstructure of the boundary layer of the LBO crystal grown in a $B_2O_3$ self-flux system. A possible mechanism is proposed to explain the crystal growth habit.

## Experimental

Fig. 1 shows the schematic diagram of our experiment system which contains two parts: a high temperature Raman

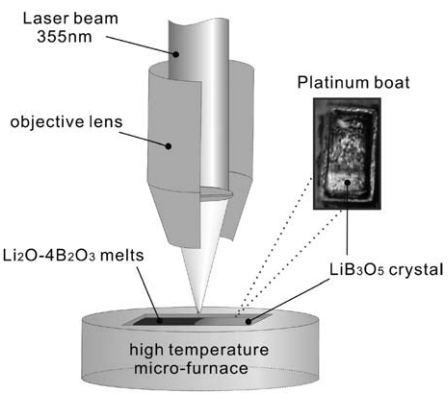


**Fig. 1** Schematic diagram of our experiment system for Raman spectroscopic measurement.

[a]*Anhui Institute of Optics and Fine Mechanics, Chinese Academy of Sciences, Hefei, 230031, China. E-mail: smwan@aiofm.ac.cn; Fax: +86 0551 5591039; Tel: +86 0551 5591039*
[b]*School of Material Science and Engineering, Shanghai University, Shanghai, 200072, China*
[c]*Technical Institute of Physics and Chemistry, Chinese Academy of Sciences, Beijing, 100080, China*

spectrometer (Jobin Y'von LABRAM HR800) and a homemade micro-furnace. The Raman spectra were recorded on the spectrometer with a backscattering configuration. The pulsed exciting light (355 nm) from a Q-switch pulsed THG-Nd:YAG laser was focused by an Olympus BH-2 microscope; the Raman scattering light from the crystal or the solution was collected by a confocal lens system. The spectral resolution was better than 2 $cm^{-1}$ and the spatial resolution was about 1 μm. The Raman spectrometer was equipped with the intensive charge-coupled device (ICCD) to observe the crystal growth process. The micro-furnace, which was specially designed to simulate the crystal growth, is composed of a sample chamber, a cooling system and a temperature controller. A platinum boat with the size of 12 mm × 7 mm × 2 mm was placed in the center of the chamber and uniformly heated by a high pure platinum wire. The maximum heating temperature can reach about 1200 °C with the precision of 1 °C.

The high-temperature solution with the composition of $Li_2O{\cdot}4B_2O_3$ is widely used to grow LBO crystal. In order to obtain the high temperature solution, a glass with the composition of $Li_2O{\cdot}4B_2O_3$ was prepared. Appropriate amounts of the starting materials, lithium carbonate and boric acid, were mixed and homogenized, and then transferred to a Pt crucible. After heating at 750 °C for one day to ensure the lithium carbonate and the boric acid decomposed completely, the temperature was slowly increased to 900 °C, and held at the temperature for 2 h to ensure the sample melted completely, then the melt was rapidly quenched. As a result, colorless $Li_2O{\cdot}4B_2O_3$ glass was obtained.

## Results and discussion

LBO crystal belongs to the orthorhombic symmetry with the space group $Pna2_1$; its basic structural unit is the triborate group ($B_3Ø_7$, Ø = bridge oxygen), a six-membered ring containing two $BØ_3$ planar triangles and one $BØ_4$ tetrahedron. The spiral chains of the $B_3Ø_7$ groups form a continuous three dimensional network; lithium cations are located in the interstices of the network.[18] Fig. 2 shows the crystal Raman spectra in the range from 200 to 1200 $cm^{-1}$ at room and high temperatures. The spectrum recorded at room temperature is in agreement with the result reported by Xiong *et al.* They considered that most of the crystal Raman peaks can be assigned to the internal vibrations of the $B_3Ø_7$ ring.[19,20] The strongest peak located at 765 $cm^{-1}$ is attributed to the symmetric breathing vibration of the ring; the strong peaks located at 1003 and 603 $cm^{-1}$ are respectively attributed to the stretching vibration of the intra-ring B–O bonds and the bending vibration of the ring; the second strongest Raman peak located at 552 $cm^{-1}$ is attributed to the stretching vibration of the $BØ_4$ tetrahedron of the ring. With the temperature increasing, all the vibrational peaks systemically shift toward low wavenumber and broaden in different degrees due to the temperature effect. No phase transition was observed, which implies LBO crystal is stable below its melting point.

Glass is a type of undercooled metastable liquid; its structure is very similar to that of the parent liquid. Investigations on the microstructure of a glass and its temperature dependent structural evolution will be helpful for us to understand the microstructure of the parent liquid. In this work, we prepared the $Li_2O{\cdot}4B_2O_3$ glass and studied its temperature-dependent structural characteristics; the results are shown in Fig. 3. The collective presence of Raman peaks located at 515, 664, 780 and 924 $cm^{-1}$ indicates that the glass is built up of a boron–oxygen network containing $B_3Ø_7$ rings, such as triborate, tetraborate or pentaborate groups.[21,22] The other strong Raman peak located at 808 $cm^{-1}$, which originates from the symmetric breathing vibration of boroxol rings ($B_3Ø_6$, a six-membered ring containing three $BØ_3$ planar triangles),[23] indicating that the $B_3Ø_6$ rings are also contained in the glass. The result has also been observed in the alkali borate glasses with low alkali cation content.[21,22,24]

With the glass melting (at about 840 °C), all of the Raman peaks broaden and shift to low wavenumber. Compared with the glass Raman spectrum, the main structural groups, $B_3Ø_6$ and $B_3Ø_7$, are still present in the melt. However, the relative intensity ratio of the 760 $cm^{-1}$ peak (the characteristic peak of $B_3Ø_7$ group) to the 790 $cm^{-1}$ peak (the characteristic peak of $B_3Ø_6$ group) decreases in the melt, which implies that a small portion of the $B_3Ø_7$ groups have changed to the $B_3Ø_6$ groups. The transformation has also been found in numerous alkali borate melts.[25–28]

For simulating LBO crystal growth by high-temperature solution method, a LBO crystal and the $Li_2O{\cdot}4B_2O_3$ glass were cut into small pieces and were respectively placed at the cool and hot sides of a platinum boat. By accurately controlling the temperature, the glass melted; new LBO crystal grew from the crystal surface. Consequently, a steady crystal–solution interface

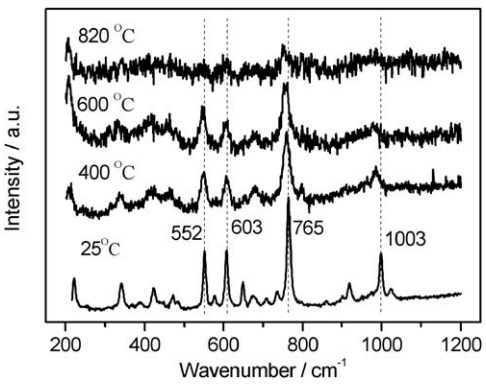


**Fig. 2** Raman spectra of LBO crystal at different temperatures.

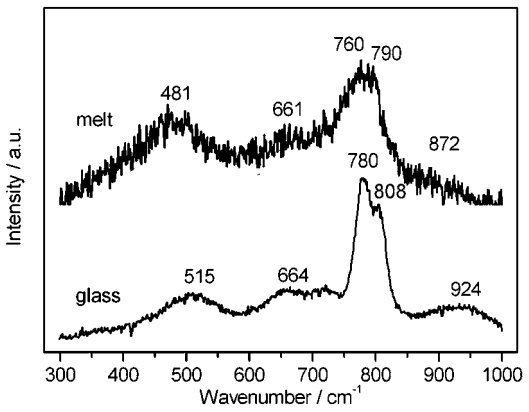


**Fig. 3** The Raman spectra of $Li_2O{\cdot}4B_2O_3$ glass (bottom) and melt (top).

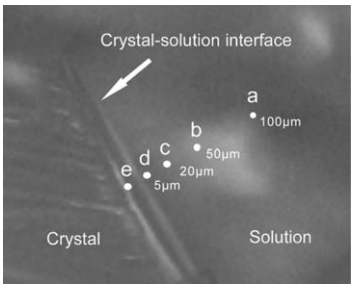


**Fig. 4** A LBO crystal–solution interface with measuring positions. The distances from the measuring position a, b, c and d to the interface are 100, 50, 20 and 5 μm, respectively. Measuring position e is on the crystal surface.

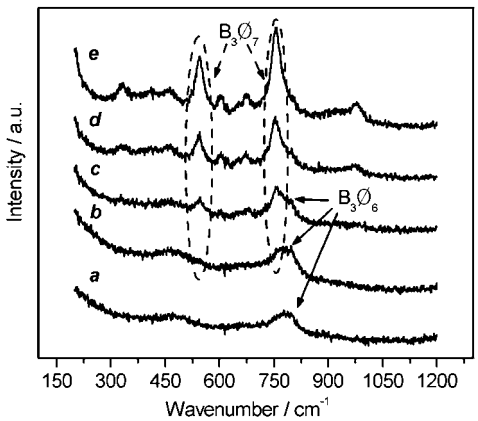


**Fig. 5** The Raman spectra recorded near the LBO crystal–solution interface. The positions of measuring points a, b, c, d and e are as shown in Fig. 4.

was produced, as shown in Fig. 4. After that, the excitation light was focused on the different positions near the crystal–solution interface to study the microstructures of the boundary layer. The measuring positions and their Raman spectra are shown in Fig. 4 and Fig. 5, respectively. The Raman spectrum recorded at position *a* is similar to that of the $Li_2O{\cdot}4B_2O_3$ melt, indicating this position has a similar microstructure with the $Li_2O{\cdot}4B_2O_3$ melt. With the measuring position moving from *b* to *d*, the Raman intensity of the peaks around 760 and 545 cm$^{-1}$ (the characteristic peaks of the $B_3Ø_7$ group) enhance gradually, while the Raman intensity of the peak around 780 cm$^{-1}$ peak (the characteristic peak of the $B_3Ø_6$ group) decreases. The result reveals that the formation of $B_3Ø_7$ groups is accompanied with the consumption of $B_3Ø_6$ groups near the crystal–solution interface. The Raman spectrum of the position *d* is very similar to that of position *e* (LBO crystal), showing that an ordered structure is formed around the crystal–solution interface.

According to the above results, we consider that an isomerization reaction between the 3- and 4-coordinated boron occurs in the boundary layer, which makes the $B_3Ø_6$ ring transform into the $B_3Ø_7$ group, as shown in Fig. 6. The reaction further leads to the increase in concentration of the $B_3Ø_7$ group near the crystal–solution interface and the formation of the quasi-ordered boundary layer whose structure is very similar to LBO crystal.

The structural evolution occurring in the boundary layer can be used to explain the growth morphology of LBO crystal. In

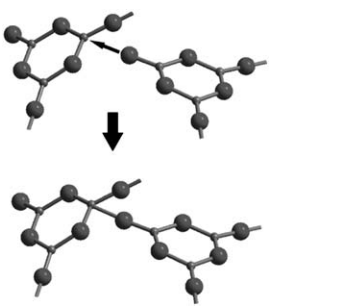

**Fig. 6** The reaction presents in the boundary layer.

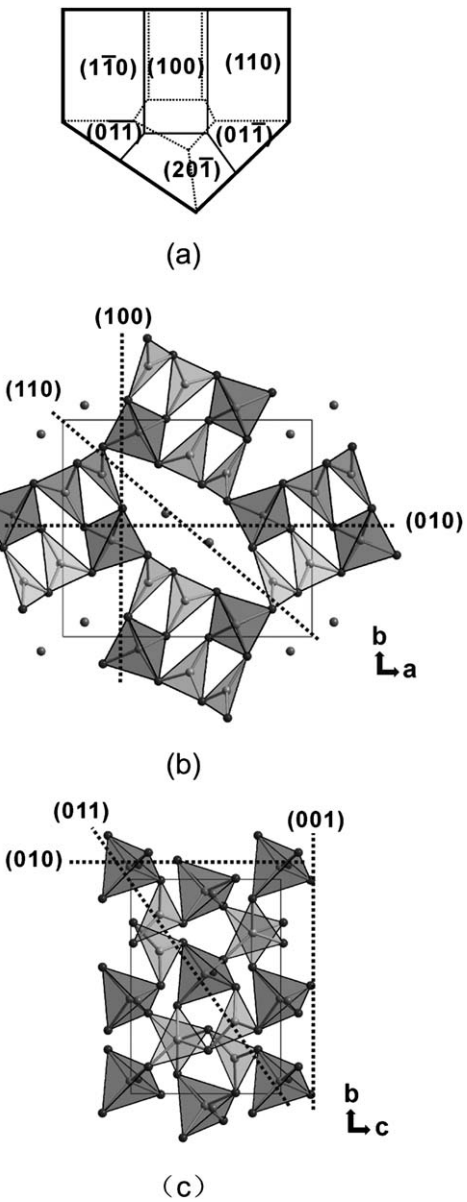


**Fig. 7** (a) The morphology of LBO crystal grown by the high-temperature solution method and the projections of the crystal structure as viewed along the *c* axis (b) and the *a* axis (c).

principle, a crystal morphology is determined by the relative growth rates of various crystal faces. The face that grows slower appears to be the larger developed face.[29] Based on the Hartman–Perdok theory,[30–32] the growth rate of a crystal face is proportional to its attachment energy ($E_{att}$, defined as the energy released when one additional growth slice of thickness $d_{hkl}$ is attached to the crystal face identified by the Miller indices *hkl*). LBO crystal growth is accompanied by the conversion from the $B_3Ø_6$ groups to the $B_3Ø_7$ groups. In this process, the $BØ_4$ tetrahedra act as the connector; therefore, the face containing more $BØ_4$ tetrahedra has a higher attachment energy and a higher growth rate; consequently, the face should be a smaller developed face. On the other hand, the face containing less $BØ_4$ tetrahedra has a lower attachment energy and a lower growth rate; the face should have a larger developed face. According to the structure of LBO crystal, we know that the $BØ_4$ densities of {011} or {201} faces are lower than that of the {001} faces. As a result, LBO crystal is expected to show well-developed {011} and {201} faces and are unlikely to exhibit {100} faces. The cases of {110}and {001} faces are shown in Fig. 7(b) and (c). The predicted results are in good agreement with the experimental results.

## Conclusions

High temperature Raman spectroscopy was applied to study *in situ* the solution microstructure near the LBO crystal–solution interface. A preordering boundary layer was found near this interface. According to the structural evolution in the boundary layer, a mechanism to describe the micro processes of LBO crystal growth is proposed. In the LBO crystal–solution boundary layers, an isomerization reaction occurs, which leads to the transformation from the $B_3Ø_6$ rings to the $B_3Ø_7$ rings, as a result, the concentration of the $B_3Ø_7$ ring increases in the boundary layer, then a boron–oxygen structure similar to LBO crystal forms near the crystal–solution interface. According to the growth mechanism, the LBO crystal growth habit can be understood very well.

## Acknowledgements

This work is financially supported by the national Natural Science Foundation of China (Grant No. 50932005) Open Project of Shanghai Key Laboratory of Modern Metallurgy and Materials Processing (Grant No. SELF-2009-01)

## Notes and references

1 P. Böni, J. H. Bilgram and W. Känzig, *Phys. Rev. A: At., Mol., Opt. Phys.*, 1983, **28**, 2953–2967.
2 S. M. Wan, X. Zhang, S. J. Zhao, Q. L. Zhang, J. L. You, L. Lu, P. Z. Fu, Y. C. Wu and S. T. Yin, *Cryst. Growth Des.*, 2008, **8**, 412–414.
3 X. Zhang, S. T. Yin, S. M. Wan, J. L. You, H. Chen, S. J. Zhao and Q. L. Zhang, *Chin. Phys. Lett.*, 2007, **24**, 1898–1900.
4 S. M. Wan, X. Zhang, S. J. Zhao, Q. L. Zhang, J. L. You, H. Chen, G. C. Zhang and S. T. Yin, *J. Appl. Crystallogr.*, 2007, **40**, 725–729.
5 S. M. Wan, B. Teng, X. Zhang, J. L. You, W. P. Zhou, Q. L. Zhang and S. T. Yin, *CrystEngComm*, 2010, **12**, 211–215.
6 P. U. Halter, J. H. Bilgram and W. Känzig, *J. Chem. Phys.*, 1988, **89**, 2622–2629.
7 J. Bilgram, *Cryst. Res. Technol.*, 1997, **32**, 1029–1039.
8 J. J. Caravajal, M. C. Pujol and F. Díaz, in *High-Temperature Solution Growth: Application to Laser and Nonlinear Optical Crystals*, ed. G. Dhanaraj, K. Byrappa, V. Prasad, M. Dudley, Springer-Verlag, Berlin, Heidelberg, 2010.
9 B. S. R. Sastry and F. A. Hummel, *J. Am. Ceram. Soc.*, 1959, **42**, 216–218.
10 B. S. R. Sastry and F. A. Hummel, *J. Am. Ceram. Soc.*, 1958, **41**, 7–17.
11 D. N. Nikogosyan, *Appl. Phys. A: Solids Surf.*, 1994, **58**, 181–190.
12 H. G. Kim, J. K. Kang, S. H. Lee and S. J. Chung, *J. Cryst. Growth*, 1998, **187**, 455–462.
13 S. A. Markgraf, Y. Furukawa and M. Sato, *J. Cryst. Growth*, 1994, **140**, 343–348.
14 D. P. Shumov, A. T. Nenov and D. D. Nihtianova, *J. Cryst. Growth*, 1996, **169**, 519–526.
15 J. W. Kima, C. S. Yoon and H. G. Gallagher, *J. Cryst. Growth*, 2001, **222**, 760–766.
16 E. Zouboulis, D. Renusch and M. Grimsditch, *Appl. Phys. Lett.*, 1998, **72**, 1–3.
17 J. L. You, G. C. Jiang and K. D. Xu, *J. Non-Cryst. Solids*, 2001, **282**, 125–131.
18 S. Zhao, C. Huang and H. Zhang, *J. Cryst. Growth*, 1990, **99**, 805–810.
19 G. S. Xiong, G. X. Lan, H. F. Wang and C. E. Huang, *J. Raman Spectrosc.*, 1993, **24**, 785–789.
20 Y. J. Jiang, Y. Wang and L. Z. Zeng, *J. Raman Spectrosc.*, 1996, **27**, 601–607.
21 B. N. Meera and J. Ramakrishna, *J. Non-Cryst. Solids*, 1993, **159**, 1–21.
22 T. W. Bril, *Philips Res. Rep. Suppl.*, 1975, **1**, 1–114.
23 F. L. Galeener, G. Lucovsky and J. C. Mikkelsen Jr, *Phys. Rev. B*, 1980, **22**, 3983–3990.
24 S. A. Feller, W. J. Dell and P. J. Bray, *J. Non-Cryst. Solids*, 1982, **51**, 21.
25 A. A. Osipov and L. M. Osipova, *Glass Phys. Chem.*, 2009, **35**, 132–140.
26 A. A. Osipov and L. M. Osipova, *Glass Phys. Chem.*, 2009, **35**, 121–131.
27 O. Majérus, L. Cormier, G. Calas and B. Beuneu, *Phys. Rev. B: Condens. Matter*, 2003, **67**, 024210.
28 K. Handa, Y. Kita, S. Kohara, K. Suzuya, T. Fukunaga, M. Misawa, T. Iida, H. Iwasaki and N. Umesaki, *J. Phys. Chem. Solids*, 1999, **60**, 1465–1471.
29 P. Hartman, in *Morphology of Crystal*, ed. I. Sunagawa, Terra, Tokyo, 1987.
30 P. Hartman and W. G. Perdok, *Acta Crystallogr.*, 1955, **8**, 49–52.
31 P. Hartman and W. G. Perdok, *Acta Crystallogr.*, 1955, **8**, 521–524.
32 P. Hartman and W. G. Perdok, *Acta Crystallogr.*, 1955, **8**, 525–529.

 